Article

Single Output and Algebraic Modal Parameters Identification of a Wind Turbine Blade: Experimental Results

Luis Gerardo Trujillo-Franco [1],*[ID]**, Hugo Francisco Abundis-Fong** [2][ID]**, Rafael Campos-Amezcua** [3][ID]**,
Roberto Gomez-Martinez** [4]**, Armando Irvin Martinez-Perez** [2]** and Alfonso Campos-Amezcua** [5]

[1] Área de Ingeniería Mecánica Automotriz, Universidad Politécnica de Pachuca, Zempoala 43830, Mexico
[2] Tecnológico Nacional de México/I.T. Pachuca, Pachuca 42080, Mexico;
hugo.af@pachuca.tecnm.mx (H.F.A.-F.); armando.mp@pachuca.tecnm.mx (A.I.M.-P.)
[3] Tecnológico Nacional de México/Centro Nacional de Investigación y Desarrollo Tecnológico,
Interior Internado Palmira S/N, Col. Palmira, Cuernavaca 62490, Mexico; rafael.ca@cenidet.tecnm.mx
[4] Instituto de Ingeniería/UNAM, Ingeniería Estructural, Ciudad de México 04510, Mexico;
rgomezm@iingen.unam.mx
[5] Instituto Nacional de Electricidad y Energías Limpias (INEEL), Av. Reforma 113, Col. Palmira,
Cuernavaca 62490, Mexico; acampos@ineel.mx
* Correspondence: luis.trujillo@upp.edu.mx

Abstract: This paper describes the evaluation of a single output, online, and time domain modal parameters identification technique based on differential algebra and operational calculus. In addition, an analysis of the frequency response function (FRF) of the system is conducted in a specific set up, emulating its nominal or operational conditions to determine the influence of the non-linearities over the dynamic behavior of the system in those particular magnitudes of deformations; thus, this influence is quantified by a numerical index. This methodology is applied to a wind turbine blade submitted to wind tunnel experiments. The natural frequencies and modal damping ratios of six bending modes associated with the blade are estimated using real-time velocity measurements from one single point of the blade. A comparison with the usual impact hammer modal testing is performed to evaluate and establish the proposed approach's main contributions. The developed modal parameter identification algorithms are implemented to run into a standard personal computer (PC) where the data acquisition system's measurements are conditioned and processed. The results show the performance and the fast parametric estimation of the proposed algebraic identification approach.

Keywords: modal analysis; modal parameters identification; algebraic identification; dynamics of wind turbine blades

1. Introduction

To ensure that wind turbine blades fulfill the design requirements, they are subjected to load-carrying capacity experimental tests under extreme loading and fatigue resistance tests. Additionally, it is common practice to perform tests to derive the blades' basic dynamic properties, such as natural frequencies and damping ratios. These are essential for the dynamic behavior and structural integrity of the entire wind turbine [1]. In this context, modal analysis is an engineering and technological tool that contributes to carry out these tests. It is also a constant topic of research and development towards new techniques and computational algorithms that lead to identifying the parameters that describe the dynamic behavior of modern engineering structures and mechanical systems [2,3]. The resulting modal models, as a product of the identification process, are used in vibration absorbers design, vibration control schemes, mechanical design, and structural health monitoring (SHM), among other important applications. Nowadays, numerous modal parameter identification algorithms, in time or frequency domain, have been reported in the literature and research articles [4–6], although most of these techniques are essentially designed to be performed in a post-processing context due to their asymptotic and recursive nature, those

methodologies are unsuitable to be applied to adaptive or real-time vibrations absorption schemes like those proposed in [7,8].

For online applications suitable to be applied in structural health monitoring and adaptive vibration control schemes, it is highly desirable to perform the parameter identification in real time, preferably online and in the nominal operation conditions of the system. Since 1996, as reported in [9], several online modal parameter identification schemes have been developed using neural networks and artificial intelligence (AI). It is also important to consider that classical mathematical models for dynamic and vibrating systems are linear assumptions of their dynamic behavior such that it is possible to use basic and well known approaches like least squares and auto-regressive models [3,10–14]. However, the use of modern materials in structural engineering, high displacements, geometrical restrictions, and complex behavior are now becoming common in modern mechanical structures, resulting in inherent non-linear phenomena (e.g., stiffness, damping, and excitation), and as a result, despite of the numerous advantages of the linearity assumption on mechanical systems, there are cases where the linear methods are no longer effective or even valid, as reported in [15–17].

In this work, we use a set of mathematical tools: Operational calculus, algebraic identification, and Hilbert transformation, to determine in time domain and online, the principal modal parameters of a wind turbine blade given one single output measurements of its free vibrations response. As a complement of our analysis, we apply the Hilbert transformation to the FRF of the system to have an indicator for the presence of non-linearities; we use the properties of this linear transformation as reported in [18] considering the interesting updates and applications reported in [17]. Then, we apply an algebraic approach to transform a complex calculus problem into an algebraic equation [19–21] in terms of the parameters to be identified. The main contributions of the present work are summarized as follows:

- An algebraic technique for online and time-domain estimation of natural frequencies and damping ratios is evaluated in an experimental case study.
- The evaluated estimation approach is performed in time-domain and on-line, where a small interval of time is required for the technique to provide accurate results.
- Compared to other modal parameters identification methods, a significant reduction of the amount of time and data required for the estimation process is the main highlight.
- Only measurements of single output signals are required. In this work, natural frequencies and damping ratios estimation are carried out using measurements of velocity.

The paper is organized as follows: In Section 2, the dynamic representation of multiple degrees of freedom mechanical systems is explained. The algebraic and online modal parameters identification scheme is detailed in Section 3. In addition, in Section 3, the mathematical fundamentals for a non-linearity analysis of the system dynamics are presented. In Section 4, the experimental work developed is presented. Finally, the most important conclusions are given in Section 5.

2. Multiple Degrees of Freedom Mechanical Systems

The vibrating mechanical system shown in Figure 1 is a schematic representation of one possible discrete form of a generic wind turbine blade considered as a mechanical structure with a finite number of degrees of freedom. It is well known that its corresponding dynamic response is determined in terms of the parameters m_i, b_{φ_i}, k_{p_i}, where the last two parameters can be expressed as a combination of a linear part and a non-linear part (viscous damping plus dry friction, Coulomb friction, etc., as well as linear stiffness plus a non-linear polynomial stiffness, duffing stiffness for example). It is important to remark that the connecting or coupling discrete elements b_{φ_i} and k_{p_i} do not follow a determined pattern or an assembling rule. The configuration shown in Figure 1 is a schematic diagram of the discrete form, considering a finite number of degrees of freedom, let it be n_{dof}.
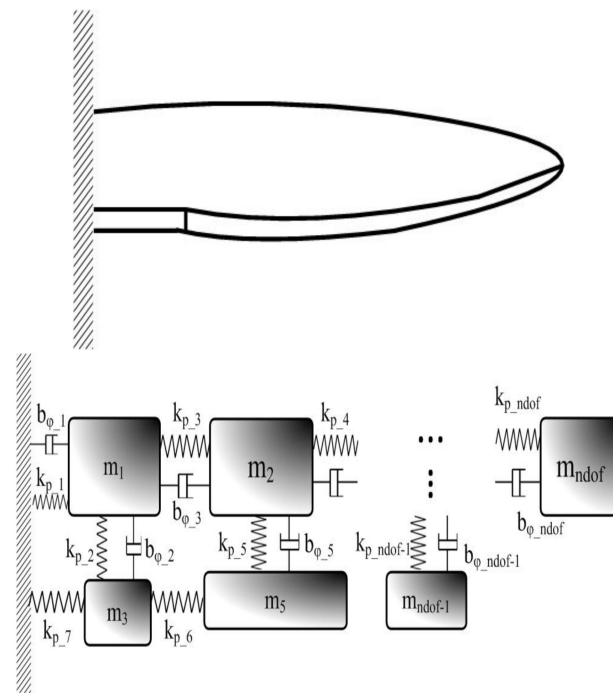
Figure 1. Generic linear/nonlinear vibrating mechanical system.

In addition to the before mentioned, let us assume that the non-linear effects can be concentrated into a function $\Phi(x, \dot{x})$, which can take a structure such that it contains or concentrates the sum of the non-linearities mentioned before. Thus, we can express the system dynamics behavior, in the conditions of free vibrations (no exogenous forces acting on the system), of this non-linear system by the following differential equation:

$$M\ddot{x} + B\dot{x} + Kx = -\Phi(x, \dot{x}) \tag{1}$$

where, the vector $x \in R^{n_{dof}}$ denotes the physical displacements of the masses as a function of time t, and the function $\Phi(x, \dot{x}) \in R^{n_{dof}}$ is a non-linear restoring force, commonly depending on the displacements and velocities of the considered n_{dof} degrees of freedom. In Equation (1), the dynamic response of the linear part is determined by the matrices $M \in R^{n_{dof} \times n_{dof}}$, $B \in R^{n_{dof} \times n_{dof}}$, and $K \in R^{n_{dof} \times n_{dof}}$, which are the mass damping and stiffness matrices, respectively, given by:

$$M = \begin{bmatrix} m_{11} & m_{12} & \cdots & m_{1n_{dof}} \\ m_{21} & m_{22} & \cdots & m_{2n_{dof}} \\ \vdots & & \ddots & \\ m_{n_{dof}1} & m_{n_{dof}2} & \cdots & m_{n_{dof}n_{dof}} \end{bmatrix}, B = \begin{bmatrix} b_{11} & b_{12} & \cdots & b_{1n_{dof}} \\ b_{21} & b_{22} & \cdots & b_{2n_{dof}} \\ \vdots & & \ddots & \\ b_{n_{dof}1} & b_{n_{dof}2} & \cdots & b_{n_{dof}n_{dof}} \end{bmatrix}$$

$$K = \begin{bmatrix} k_{11} & k_{12} & \cdots & k_{1n_{dof}} \\ k_{21} & k_{22} & \cdots & k_{2n_{dof}} \\ \vdots & & \ddots & \\ k_{n_{dof}1} & k_{n_{dof}2} & \cdots & k_{n_{dof}n_{dof}} \end{bmatrix} \tag{2}$$

As mentioned before, it is common for the non-linear restoring force to assume a structure such that it contains the sum of non-linearities like dry friction, non-linear damping, and some polynomial stiffness as follows [18]:

$$\Phi(x, \dot{x}) = K_{ip}x^r + K_{(i-1)p}x^{r-1} + \cdots + K_{2p}x^2 + F_d\text{sign}(x) + C_d\text{sign}(\dot{x}) \tag{3}$$

where r is the order or the polynomic stiffness, and $K_{ip} \in R^{n_{dof} \times n_{dof}}$ are the polynomial stiffness matrices, with $i = 2, 3, ..., r$ given by:

$$K_{ip} = \begin{bmatrix} k_{ip_{11}} & k_{ip_{12}} & \cdots & k_{ip_{1n_{dof}}} \\ k_{ip_{21}} & k_{ip_{22}} & \cdots & k_{ip_{2n_{dof}}} \\ \vdots & & \ddots & \\ k_{ip_{n_{dof}1}} & k_{ip_{n_{dof}2}} & \cdots & k_{ip_{n_{dof}n_{dof}}} \end{bmatrix}, \quad i = 2, 3, ..., r \tag{4}$$

The matrices $F_d \in R^{n_{dof} \times n_{dof}}$ and $C_d \in R^{n_{dof} \times n_{dof}}$ are the Coulomb dry friction and nonlinear damping matrices, respectively, with the following structure.

$$F_d = \begin{bmatrix} f_{d11} & f_{d12} & \cdots & f_{d1n_{dof}} \\ f_{d21} & f_{d22} & \cdots & f_{d2n_{dof}} \\ \vdots & & \ddots & \\ f_{dn_{dof}1} & f_{dn_{dof}2} & \cdots & f_{dn_{dof}n_{dof}} \end{bmatrix}, C_d = \begin{bmatrix} c_{d11} & c_{d12} & \cdots & c_{d1n_{dof}} \\ c_{d21} & c_{d22} & \cdots & c_{d2n_{dof}} \\ \vdots & & \ddots & \\ c_{dn_{dof}1} & c_{dn_{dof}2} & \cdots & c_{dn_{dof}n_{dof}} \end{bmatrix} \tag{5}$$

For the traditional modal analysis approaches [2,3,6,22–24], it is crucial that $\Phi(x, \dot{x}) \approx 0$ for the correct performance of the identification methods, when $\Phi(x, \dot{x}) \neq 0$, the classic modal analysis tools are inoperative or inaccurate. This situation demonstrates the need to have an indicator of how important or dominant the non-linear terms are over the global dynamic response of the system. In the following section, we present the application of a mathematical method for determining this influence in terms of a numerical indicator.

3. Algebraic and Online Modal Parameters Identification

Consider, as mentioned in the last section, that the mechanical system shown in Figure 1 is a general graphic representation of a wind turbine blade, whose dynamic response can be determined by Equation (1). The classic experimental modal analysis paradigm for mechanical engineering is to consider that the influence of the non-linear part can be neglected, that is, $\Phi(x, \dot{x}) \approx 0$ or, in the best case, it is such that: $\Phi(x, \dot{x}) \equiv 0$. When possible, considering the dynamic behavior of the system as linear results in an uncoupled $2n_{dof}$ grade, which can be expressed in terms of the principal or generalized coordinates [3] q_i as follows:

$$\ddot{q}_i + 2\xi_i \omega_{ni} \dot{q}_i + \omega_{ni}^2 q_i = 0$$
$$x(t) = \Psi q(t) \tag{6}$$

where ω_{ni} and ξ_i are the natural frequencies and damping ratios associated with the i-th vibration mode, respectively, and Ψ is the modal matrix with components ψ_{ij} that contains the column space of the eigenvectors of the system (1) given by

$$\Psi = \begin{bmatrix} \psi_{11} & \psi_{12} & \cdots & \psi_{1n_{dof}} \\ \psi_{21} & \psi_{22} & \cdots & \psi_{2n_{dof}} \\ \vdots & & \ddots & \\ \psi_{n_{dof}1} & \psi_{n_{dof}2} & \cdots & \psi_{n_{dof}n_{dof}} \end{bmatrix} \tag{7}$$

In notation of the Mikusiński's operational calculus [20,21], the modal analysis representation or modal model (6) is:

$$(s^2 + 2\xi_i \omega_{ni} s + \omega_{ni}^2) q_i = 0 \tag{8}$$

The combination of Equations (6) and (8) leads to

$$x_i(s) = \sum_{j=1}^{n_{dof}} \frac{\psi_{ij}(\alpha_{0,i} + \alpha_{1,i}s)}{(s^2 + 2\xi_i\omega_{ni}s + \omega_n{}^2)} \tag{9}$$

where the constants $\alpha_{0,i}$ and $\alpha_{1,i}$ depend on the initial conditions. Therefore, the physical displacements x_i are given by

$$p_c(s)x_i(s) = \rho_{0i} + \cdots + \rho_{1i}s + \rho_{2n_{dof}-1i}s^{2n_{dof}-1} \tag{10}$$

with:

$$p_c(s) = s^{2n_{dof}} + a_{2n_{dof}-1}s^{2n_{dof}-1} + \ldots + a_3s^3 + a_2s^2 + a_1s + a_0 \tag{11}$$

where $p_c(s)$ is the characteristic polynomial of the vibrating mechanical system, ρ_{ij} are constants that depend on the initial conditions and the modal matrix components ψ_{ij}. The components of the characteristic polynomial (11) provide the damping factors and damped natural frequencies, and hence, the natural frequencies and damping ratios of the flexible structure. Moreover, since the characteristic polynomial of the system is unique, it does not make any difference in which output x_i is selected.

Note that the mathematical model (1) can describe any *N* DOF vibrating mechanical system, with *N* being an arbitrarily large integer. In previous works, the direct parameter identification of the system parameters such as mass, stiffness, and damping ratios have been realized using algebraic parameter identification methods as described in [20,25], where some comparisons with ARX and ARMAX methods are discussed, consequent works as [26,27] report the modal parameters identification schemes, evaluated in time domain and online. In this work, we propose a reliable extension of those algebraic parameter identification methods [20,26,27] for general *N* DOF modal models. Herein, $n_{dof} < N$ is the number of degrees of freedom to be considered, and the parameters a_i belong to the characteristic polynomial of the system. The components of this polynomial contain the modal parameters of the system ω_i and ξ_i.

As reported in [20,25–27], the general expression for the proposed time domain, algebraic identification scheme for modal parameters in the case of multiple degrees of freedom, is given by

$$\Theta = G^{-1}V = \frac{1}{\Delta}\begin{bmatrix} \Delta_1 \\ \Delta_2 \\ \vdots \\ \Delta_n \end{bmatrix} \tag{12}$$

where the vector $\Theta = [\hat{a}_{2n_{dof}-1} \cdots \hat{a}_1 \ \hat{a}_0]^T$ contains the estimated coefficients of the characteristic polynomial and Δ is the determinant of the matrix G and Δ_i, which are partial determinants used for the Cramer's rule. The matrix $G \in R^{2n_{dof} \times 2n_{dof}}$ and the vector $V \in R^{2n_{dof}}$ are given by

$$G = \begin{bmatrix} g_{11} & g_{12} & \cdots & g_{12n_{dof}} \\ g_{21} & g_{22} & \cdots & g_{22n_{dof}} \\ \vdots & & \ddots & \\ g_{2n_{dof}1} & g_{n_{dof}2} & \cdots & g_{2n_{dof}2n_{dof}} \end{bmatrix}, V = \begin{bmatrix} v_1 \\ v_2 \\ \vdots \\ v_{2n_{dof}} \end{bmatrix} \tag{13}$$

with entries defined by

$$
\begin{aligned}
g_{11} &= (-1)^{2n_{dof}} \int_{t_0}^{2n_{dof}} (\Delta t)^{(2n_{dof})} x_i(t) \\
g_{12} &= \sum_{k=0}^{1} (-1)^{2n_{dof}-k} \frac{(2n_{dof})!(1)!}{k!(2n_{dof}-k)!(1-k)!} \int_{t_0}^{(2n_{dof}-1+k)} (\Delta t)^{2n_{dof}-k} x_i(t) \\
\vdots &= \qquad\qquad \vdots \\
g_{1,2n_{dof}-1} &= \sum_{k=0}^{2n_{dof}-2} \beta_k \int_{t_0}^{(2+k)} (\Delta t)^{(2n_{dof}-k)} x_i(t) \\
g_{1,2n_{dof}} &= \sum_{k=0}^{2n_{dof}-1} \gamma_k \int_{t_0}^{(1+k)} (\Delta t)^{(2n_{dof}-k)} x_i(t)
\end{aligned}
\tag{14}
$$

where $x_i(t)$ is a single available output measurement. Notice that none of Equation (15)'s expressions depend on the initial conditions of the considered output $x_i(t)$. In (15), $\Delta t = t - t_0$, and the notation $\int_{t_0}^{(k)} \varphi(t)$ represents iterated integrations of the form

$$
\int_{t_0}^{t} \int_{t_0}^{\tau_1} \cdots \int_{t_0}^{\tau_{k-1}} \varphi(\tau_k) d\tau_k \cdots d\tau_1
\tag{15}
$$

where k is a positive integer. The constants β_k, γ_k used in (15) are defined as

$$
\beta_k = (-1)^{2n_{dof}-k} \frac{(2n_{dof})!(2n_{dof}-2)!}{k!(2n_{dof}-k)!(2n_{dof}-2-k)!}
\tag{16}
$$

$$
\gamma_k = (-1)^{2n_{dof}} \frac{(2n_{dof})!(2n_{dof}-1)!}{k!(2n_{dof}-k)!(2n_{dof}-1-k)!}
$$

Finally, the first element v_1 of the vector $V = [v_1 \ v_2 \cdots v_{n_{dof}}]$, defined in Equation (13), is obtained as follows

$$
v_1 = - \sum_{k=0}^{2n_{dof}-1} \lambda_k \int_{t_0}^{(k)} (\Delta t)^{(2n_{dof}-k)} x_i(t)
\tag{17}
$$

where the constants λ_k are calculated by using the expression

$$
\lambda_k = (-1)^{2n_{dof}-k} \frac{(2n_{dof})!(2n_{dof})!}{k!(2n_{dof}-k)!(2n_{dof}-k)!}
\tag{18}
$$

The iterated integrations of Equations (15) and (17) lead to the rest of the entries or components of the matrix G and the vector V

$$
g_{ij} = \int_{t_0} g_{i-1j}, \quad v_i = \int_{t_0} v_{i-1}
\tag{19}
$$

with $i = 2, \ldots, 2n_{dof}$ and $j = 1, \ldots, 2n_{dof}$. It is possible to estimate the desired coefficients by using Cramer's rule. The iterated integration m times of the numerator and denominator leads to smooth estimations with the consequent slower convergence of the calculations. Let us rewrite Equation (12) with no changes in the final result as

$$
e^{-\gamma(t-t_0)} |\Delta| \hat{a}_k = e^{-\gamma(t-t_0)} \begin{bmatrix} |\Delta_1| \\ |\Delta_2| \\ \vdots \\ |\Delta_n| \end{bmatrix}
\tag{20}
$$

$$\hat{a}_k = \frac{e^{-\gamma(t-t_0)} \int_{t_0}^{(m)} |\Delta_{k-1}|}{e^{-\gamma(t-t_0)} \int_{t_0}^{(m)} |\Delta|}, \quad k = 1, 2, \cdots, 2n_{dof} - 1 \tag{21}$$

where $|\cdot|$ denotes absolute value, m is an integer, $\hat{}$ denotes estimated, and $\gamma_1 > 0$ is a low-pass filter coefficient used to smooth the online estimations [28]. Thus, from the algebraic estimation of the coefficients $\hat{a}_k$, it is possible to obtain the components of the characteristic polynomial and, hence the natural frequencies and damping ratios, as reported in [26]

$$\hat{r}_i = \hat{\varsigma}_i + j\hat{\omega}_{di}, \quad \hat{r}_i^* = \hat{\varsigma}_i - j\hat{\omega}_{di}, \quad i = 1, 2, \cdots, n_{dof} \tag{22}$$

here, $\hat{\varsigma}_i$ and $\hat{\omega}_{di}$ are the estimates of the damping factors and damped natural frequencies, respectively. Consequently, the estimates of the natural frequencies and damping ratios are given by

$$\hat{\omega}_{ni} = \sqrt{\hat{\varsigma}_i^2 + \hat{\omega}_{di}^2}, \quad \hat{\xi}_i = -\frac{\hat{\varsigma}_i}{\sqrt{\hat{\varsigma}_i^2 + \hat{\omega}_{di}^2}} \tag{23}$$

It is important to remark that this identification approach can also be extended to the case of velocity measurements, available with laser vibrometry, by multiplying Equation (24) by the complex variable s so we can describe a velocity output as

$$vel_i(s) = \sum_{j=1}^{n_{dof}} \frac{\psi_{ij}(\alpha_{0,i}s + \alpha_{1,i}s^2)}{(s^2 + 2\xi_i\omega_{ni}s + \omega_n^2)} \tag{24}$$

where $vel_i(s) = sx_i(s)$ is a particular and available velocity output test point in the complex domain s, and then, it is possible to follow the proposed identification methodology as reported in [26], and experimentally verified in [27], where the algebraic identification approach was evaluated for the particular case of acceleration measurements. Finally, to depict the proposed approach graphically, we present a block diagram in Figure 2 that describes the corresponding process of the algebraic identification of parameters. The proposed algebraic and on-line modal parameters identification scheme is limited to determining two modal parameters, natural frequencies, and modal damping ratios.
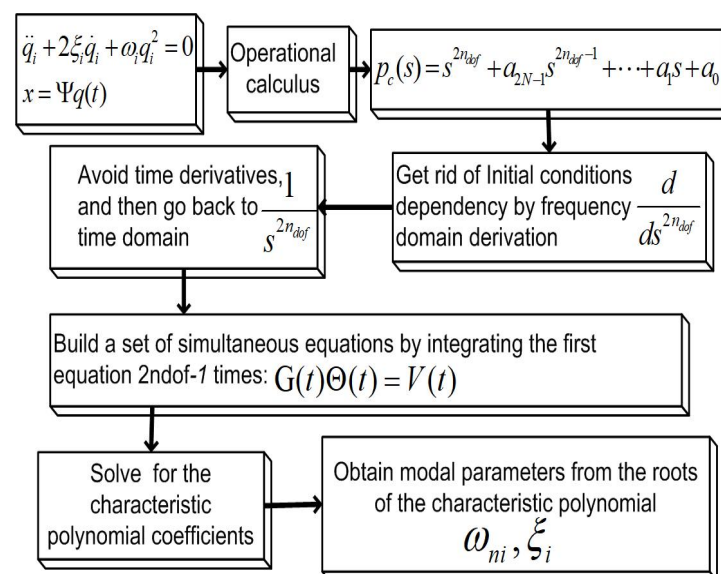

Figure 2. Algebraic identification approach.

Non-Linearity Analysis

In order to enhance the reliability of the modal parameters identification scheme proposed here, it is important to verify the presence of the significant non-linearities in the

inherent system dynamic response that could compromise the performance of the algebraic identifier (21). Even though the algebraic identification technique has been numerical and experimentally verified for non-linear mechanical systems, see [20,29], the main aim of this work is to analyze the linear part of the dynamic response for modal parameters identification purposes. To achieve this particular objective, there are numerical methods for determining the influence of non-linearities present in the system dynamics, and these methods are well reported in [17] and references therein. Despite the numerous advantages of the linearity assumption on mechanical systems, there exist cases where the linear methods are ineffective or inoperative; therefore, we need to analyze and quantify the presence of non-linearities on the particular mechanical system numerically.

The Hilbert transformation [18,29,30] is a popular and well-founded mathematical tool widely used to analyze the dynamic behavior of mechanical systems due to its particular properties when it is applied to experimental frequency response functions. Since the Hilbert transform maps the functions under consideration into the same domain, when applying the Hilbert transform to a FRF, let it be $\mathcal{R}(j\omega)$, then, the imaginary and the real parts of the FRF are related as follows:

$$Re(\mathcal{R}(j\omega)) = -\frac{1}{\pi}\eta \int_{-\infty}^{\infty} \frac{Im(\mathcal{R}(j\omega))}{\omega - \omega_c} dj\omega \tag{25}$$

$$Im(\mathcal{R}(j\omega)) = \frac{1}{\pi}\eta \int_{-\infty}^{\infty} \frac{Re(\mathcal{R}(j\omega))}{\omega - \omega_c} dj\omega \tag{26}$$

where $j = \sqrt{-1}$ and η denotes the Cauchy principal value of the integral, which is necessary to consider due to the singularity of (25) and (26) present at $\omega = \omega_c$. The equations or relations (26) and (25) are known as the Hilbert transform pairs [18,30]. It is well known that, for non-linear systems, the pairs do not comply and the Hilbert transform will return a distorted version of $\mathcal{R}(j\omega)$. As a result, we have a non-linearity indicator by analyzing the level of distortion on the original FRF $\mathcal{R}(j\omega)$ by using cross-correlation as follows:

$$\sigma_{\mathcal{H}} = \|Q_{\mathcal{HR}}(0)\|^2 \tag{27}$$

where $\|Q_{\mathcal{HR}}(0)\|$ is the normalized cross-correlation coefficient and $Q_{\mathcal{HG}}$ is given by

$$Q_{\mathcal{HR}}(\Delta j\omega) = \int_{-\infty}^{\infty} \mathcal{H}(j\omega)\mathcal{R}(j\omega + \Delta j\omega) dj\omega \tag{28}$$

where $\mathcal{R}(j\omega)$ is the original FRF of the system and $\mathcal{H}$ is the Hilbert transformation of $\mathcal{R}$. This coefficient is a numerical indicator of the non-linear behavior of the system at a specific amplitude of the input force. We use this index to study the presence of non-linearities in the system under study, such that when $\sigma_{\mathcal{H}}$ diverges from 1, the system shows a behavior that is mainly non-linear; that is, for a linear system, the expected value of $\sigma_{\mathcal{H}}$ is precisely 1. It is important to consider that the Hilbert transform is a numerical method; then, we need to consider some linearity criterion. Therefore, as reported in [17,29,30], we can consider the set of values $0.9 \leq \sigma_{\mathcal{H}} \leq 1$ for a linearity assumption of the dynamic behavior of the system.

4. An Experimental Case Study

The proposed modal parameters estimation scheme was evaluated on a fiberglass wind turbine blade. First, a traditional impact test modal analysis was conducted to determine the presence of non-linearities due to the inherent nature of the composite material used for the base of the blade. Simultaneously, by performing a traditional modal testing on the blade, a reference is obtained and used to evaluate the performance of the proposed scheme. Figure 3 shows the experimental set-up for the traditional modal testing. Two different modal parameter extraction techniques were applied to the experimental data; the classic one degree of freedom peak picking method detailed in [3], and the

multiple degrees of freedom rational fractional polynomials method, known as RFP and reported in [31].

Figure 3. Blade set-up for modal testing based on impact hammer excitation.

Figure 3 shows a clamped free blade used to match boundary conditions for operational conditions of the blade when the brake is applied. The test was performed using single output velocity measurements employing a laser vibrometer model PDV-100 and its corresponding data acquisition hardware connected via USB to a laptop computer. The measured FRF corresponding to velocity measurements of one single output or degree of freedom is shown in Figure 4, where only the first six resonances are considered. The curve in the solid blue line corresponds to the experimental FRF, while the dotted red and black lines correspond to synthesized FRFs obtained by applying the peak picking [3] and RFP methods [2,31,32], respectively.
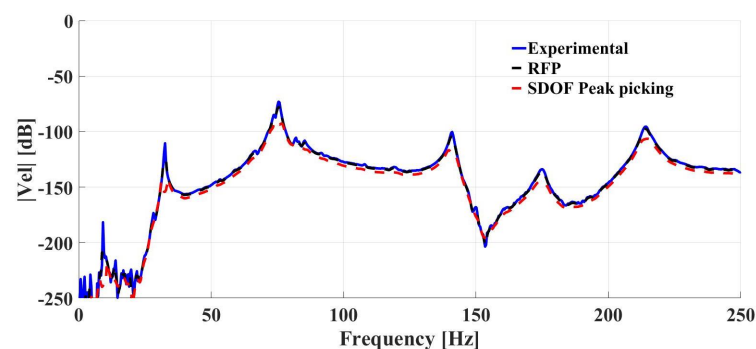

Figure 4. FRF (frequency response function) of the velocity measurements.

Notice that the first modes are difficult to detect and analyse in the frequency domain, even though the deflection of the blade at low frequencies is evident. A second impact hammer test was performed using IEPE accelerometer sensors to compare and validate the former test results. The corresponding FRF for the acceleration measurements case is shown in Figure 5, where the two first bending modes are easily located at a low frequency band [33].
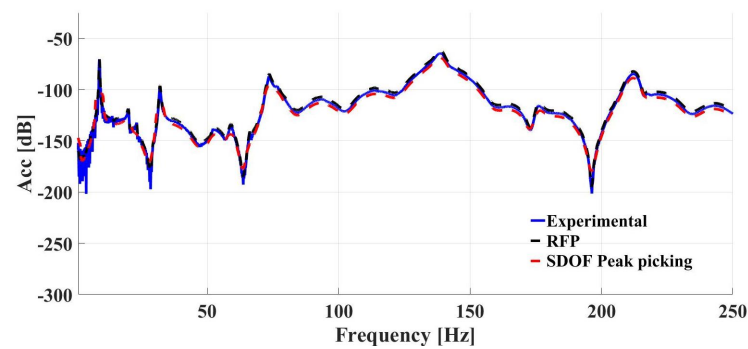
Figure 5. FRF of the acceleration measurements.

In Figure 6, the first 6 modal shapes are shown in a three-dimensional graph. The different deformation patterns were obtained using the traditional impact hammer test described in the literature [3], in six different points of the blade, uniformly spaced. In addition, one point was taken as a reference. In the plane perpendicular to the deformation, the first six modes of vibration are shown in Figure 7, while the corresponding modal vectors obtained are reported in Table 1.
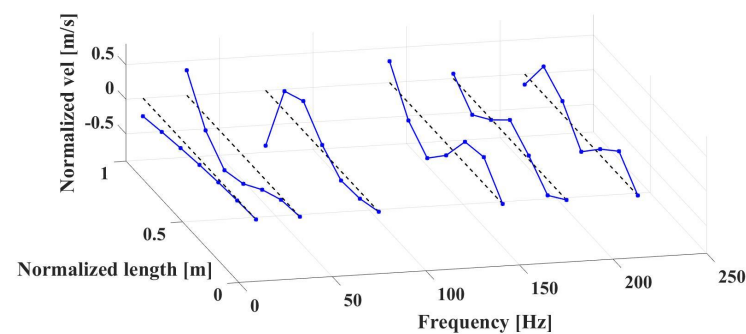

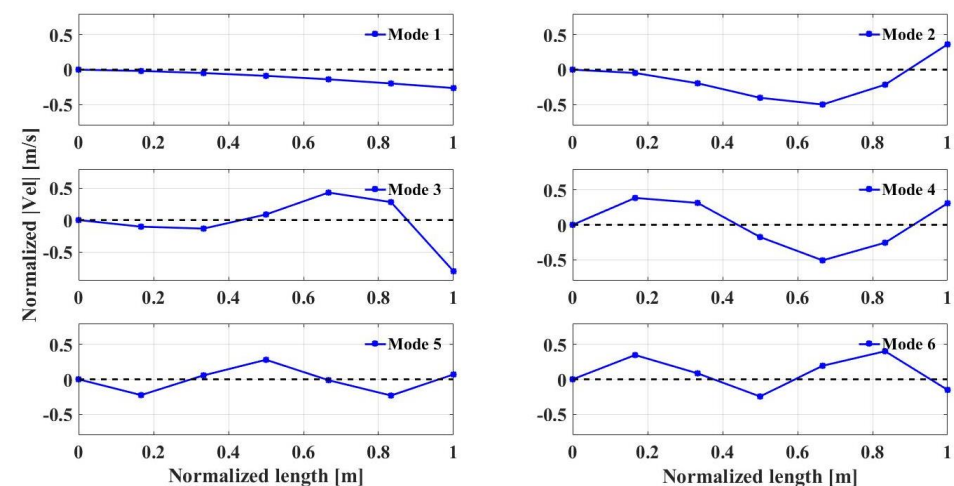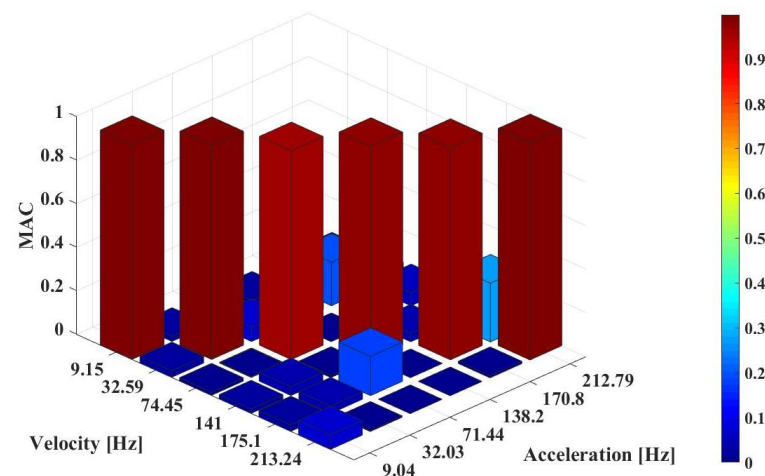**Figure 6.** Graph of the six bending modes at six first resonant frequencies.

Figure 7. First six bending mode shapes of the blade.

Table 1. Normalized modal vectors.

Test Point	Mode 1	Mode 2	Mode 3	Mode 4	Mode 5	Mode 6
1	−0.0189	−0.0480	−0.1040	0.3852	−0.2265	0.3477
2	−0.0487	−0.1956	−0.1342	0.3141	0.0564	0.0851
3	−0.0890	−0.4033	0.0873	−0.1753	0.2796	−0.2464
4	−0.1389	−0.4995	0.4308	−0.5095	−0.0129	0.1940
5	−0.1976	−0.2155	0.2811	−0.2561	−0.2325	0.4023
6	−0.2637	0.3627	−0.8022	0.3088	0.0696	−0.1520

Remark: It is important to clarify that the reported results are the product of a traditional experimental modal analysis, whose objective is to provide the parameters that serve as a reference to make a comparison of the performance of the proposed online algebraic estimator defined by (21) and (23). The modal shapes were obtained through the excitation technique by using an impact hammer and the synthesis of FRFs employing the methods of extraction of modal parameters peak picking and rational fractional polynomials RFP [2,3,31,32].

The modal assurance criterion known as MAC [33] is a graphic indicator used to indicate the degree of consistency or similarity between modes obtained by two different methods. The expected value of the MAC between two consistent modes is 1. In Figure 8, the modal assurance criterion for the modes obtained by the two sets of measurements, velocity and acceleration, is graphically shown. It is clear to verify the consistency of the data obtained from both tests.

Figure 8. Modal Assurance Criterion (MAC).

In order to determine the influence of non-linearities in the dynamic response of the blade, Hilbert transform analysis of the velocity FRF was performed. First, we apply the Hilbert transform algorithm to the original FRF, and then we compare both of the FRFs to find possible distortions. The resulting transformation is shown in Figure 9, where the original FRF is shown in a continuous blue line and the transformation in bold black. The zoom in the three-dimensional chart in Figure 9 shows the low distortion level for the range of the second resonant frequency. A visual inspection of Figure 9 confirms that the original FRF does not present an important distortion after applying the Hilbert transformation; therefore, we can consider the blade as a linear system under these excitation and deflection amplitudes. The proposed non-linearity index expressed in Equation (27) is:

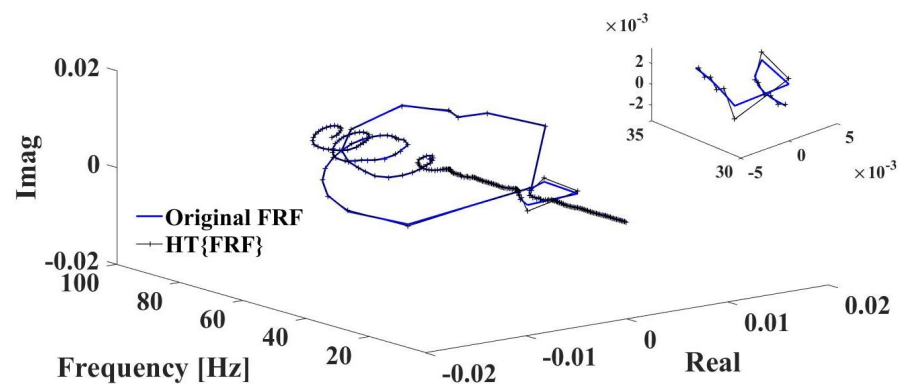$$\sigma_{\mathcal{H}} = \|R_{\mathcal{HR}}(0)\|^2 = 0.93 \tag{29}$$

Figure 9. Original FRF (blue line) and its corresponding Hilbert transformation with first mode detail.

The Argand diagram of the FRF and its Hilbert transformation is shown in Figure 10, where the original response is depicted in a blue and continuous line. In contrast, the corresponding Hilbert transformation is represented in a bold black line.
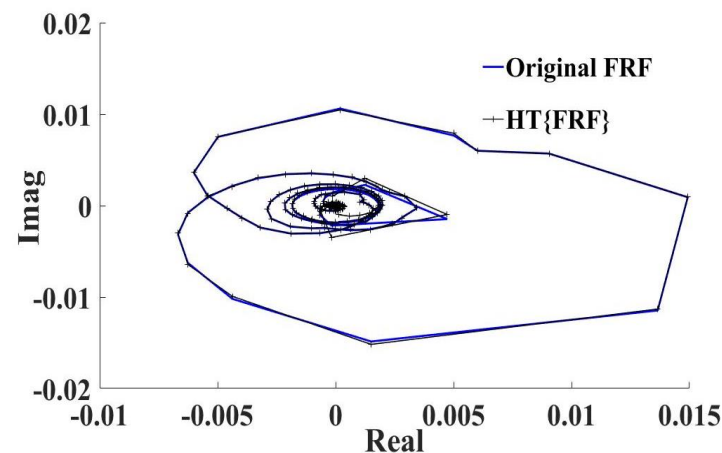

Figure 10. Argand diagram of the original FRF (blue continuous line) and its Hilbert transformation (black marked line).

The averaged modal parameters estimated by the traditional rational fractional polynomials and peak picking techniques are reported in Table 2 for the first six bending vibration modes.

Table 2. Offline modal parameters estimation, averaged peak picking, and rational fractional polynomial (RFP) methods.

Mode	Frequency [Hz]	Damping Ratio %
1	9.15	1.5
2	32.59	0.9
3	74.75	1.43
4	141.0	2.8
5	175.1	2.0
6	213.24	1.8

The modal parameters reported in Table 2 were obtained by applying the traditional and experimental modal analysis techniques that are inherently offline and frequency domain. Those experimental techniques are reported in [2,3,31,32]. Those parameters are used as a comparative reference for evaluating the performance of the online and algebraic approach for the first six bending vibration modes.

Moreover, based on the results obtained with the application of the non-linearity index, whose numerical value is $\sigma_{\mathcal{H}} = 0.93$, it is perfectly valid to use the velocity measurements of the analyzed output for the synthesis of the algebraic identifier (21), given that the dynamic behavior of the blade is dominantly linear and, as a consequence, the condition $\Phi(x, \dot{x}) \approx 0$ is satisfied.

Wind Tunnel Experiments

Experiments were carried out in the atmospheric boundary layer wind tunnel of the Institute of Engineering of the National Autonomous University of Mexico and FiiDEM Alliance. The 2 m high and 3 m wide test section has two rotary tables separated by 14 m. The 5.5×5.5 m contraction at the inlet nozzle, together with a series of honeycomb and a set of fine-grid screens, allows a remarkably low turbulence level ($I < 1\%$). The flow is accelerated at a velocity between 0.2 m/s and 30 m/s in a closed-loop configuration. Figure 11 shows a schematic view of the test section. Rotary Table 2 was used for the measurements.
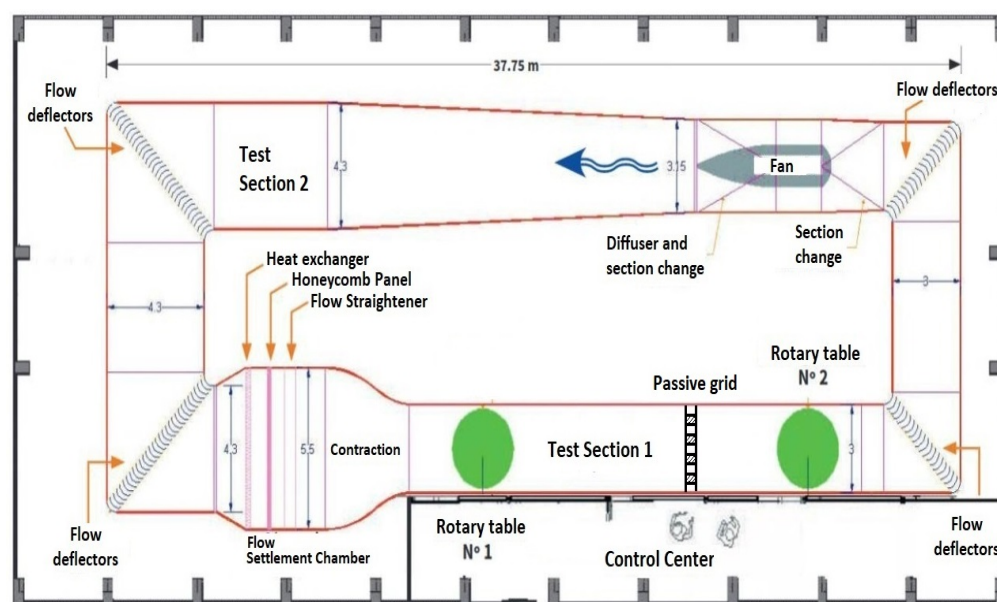

Figure 11. Atmospheric boundary layer wind tunnel of the II-UNAM and FiiDEM Alliance. The experiments were carried out in rotary table 2; the passive grid was fixed to 5 m upstream of the rotary table 2.

In the first instance, a test was carried out considering laminar flow conditions; however, the dynamic behavior of the blade was not observed. Subsequently, a specially designed grid was used to generate a turbulent flow, which is produced by the shedding of vortices downstream of the bars. The grid characteristics are the following; the width of the bars $b = 5$ cm, mesh size $M = 35$ cm (i.e., the distance between the centreline of the bars), and the downstream distance from the grid to the section where measurements were performed $x = 5$ m, see Figure 12. The $x/M > 14$ rate assures a homogeneous and isotropic turbulent flow [34], whose main characteristics are a turbulence intensity of $I = 4.2\%$ and an integral length $L = 0.2$ m.

In a second instance, in order to the evaluate the proposed algebraic identifier of Equation (21), we exposed the wind turbine blade to turbulent flow conditions with a wind speed of 20 m/s in a time span of 0–18 s. At this point, the wind tunnel fan was turned off to generate a free decay response for the interval of 18–40 s, which is then used to synthesize the on-line algebraic identifier (21). Turbulence was generated by placing a fixed pattern grid in front of the blade, as shown in Figure 12, where the measured point on the blade is the same that we used for impact hammer testing.

Figure 12. Experimental set-up for wind tunnel experiments: passive grid, blade, and laser vibrometer.

Time-domain velocity measurements are shown in Figure 13. After 18 s of running the test, as shown on the right side of Figure 13, the fan of the wind tunnel was powered off to generate the free vibrations condition for the blade; at this moment, the algebraic identifier is engaged to estimate in an online fashion the natural frequencies and damping ratios of the first six modes of the blade.
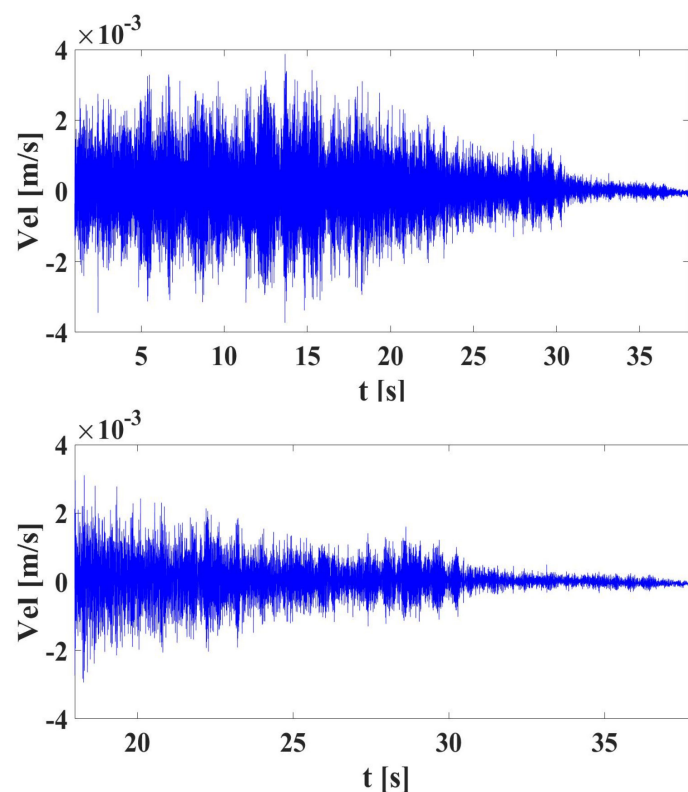

Figure 13. Free decay response in time domain. Complete experiment and decay with fan turned off.

In order to derive a method to determine the moment when the algebraic estimator converges to stable calculations, we propose to use a sentinel variable that has a known value of 1, as shown in Figure 14. This unitary variable comes from the characteristic polynomial (11), where the $N - th$ power coefficient of the complex variable s precisely equals 1.
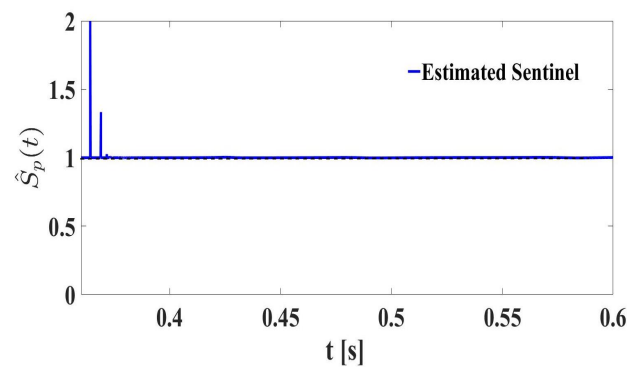
Figure 14. Convergence of the sentinel parameter.

The fast and online estimations of the modal parameters are shown in Figures 15 and 16, where the dotted line is the numerical value obtained by the classic off-line peak picking and RFP techniques. Notice that it takes less than a second for the algebraic identifier to give smooth and stable estimations of the modal parameters obtained by solving the roots of the estimated characteristic polynomial of coefficients $\hat{a}_k$. Results of the online modal parameters estimation are reported in Table 3, in addition, the results obtained by the traditional off-line peak picking and RFP methods are compared to the results obtained with the time domain and online algebraic technique.

The performance of the evaluated algebraic identifier implies the effective, online, and time-domain determination of two important modal parameters of the system; natural frequencies and damping ratios. As reported in important and interesting contributions [15,16] on structural health monitoring (SHM), the effective detection of changes in these modal parameters results in a reliable indication of the physical conditions of the systems under analysis. In addition, a desirable feature of structural monitoring techniques is a fast performance with a limited number of sensors and as little post-processing as possible. The identification scheme evaluated in this work achieves those characteristics and is feasible for its application in real-time and online structural monitoring schemes.

Finally, the real time and online determination of the mode shapes with the evaluated algebraic scheme, will be a natural extension, part of future works, in the context of structural health monitoring (SHM) applications.

Table 3. Results summary and comparison.

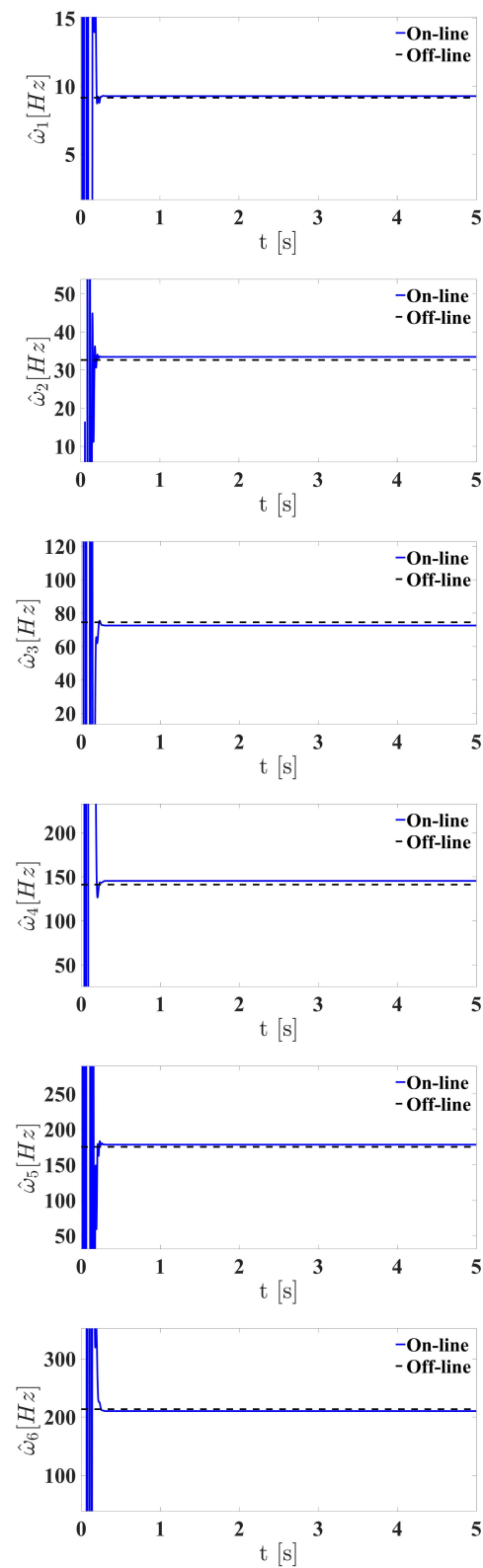|	Frequency [Hz]		
Mode	**Off-Line**	**On-Line**	**Difference %**
1	9.15	9.26	1.29
2	32.59	33.40	2.51
3	74.45	72.51	2.6
4	141.0	145.23	3.0
5	175.1	178.25	1.8
6	213.24	210.04	1.5
	Damping Ratio %		
Mode	**Off-Line**	**On-Line**	**Difference %**
1	1.5	1.55	2.9
2	0.9	0.85	5.1
3	1.43	1.25	1.26
4	2.8	2.88	3.0
5	2.0	2.16	7.8
6	1.8	1.74	3.5

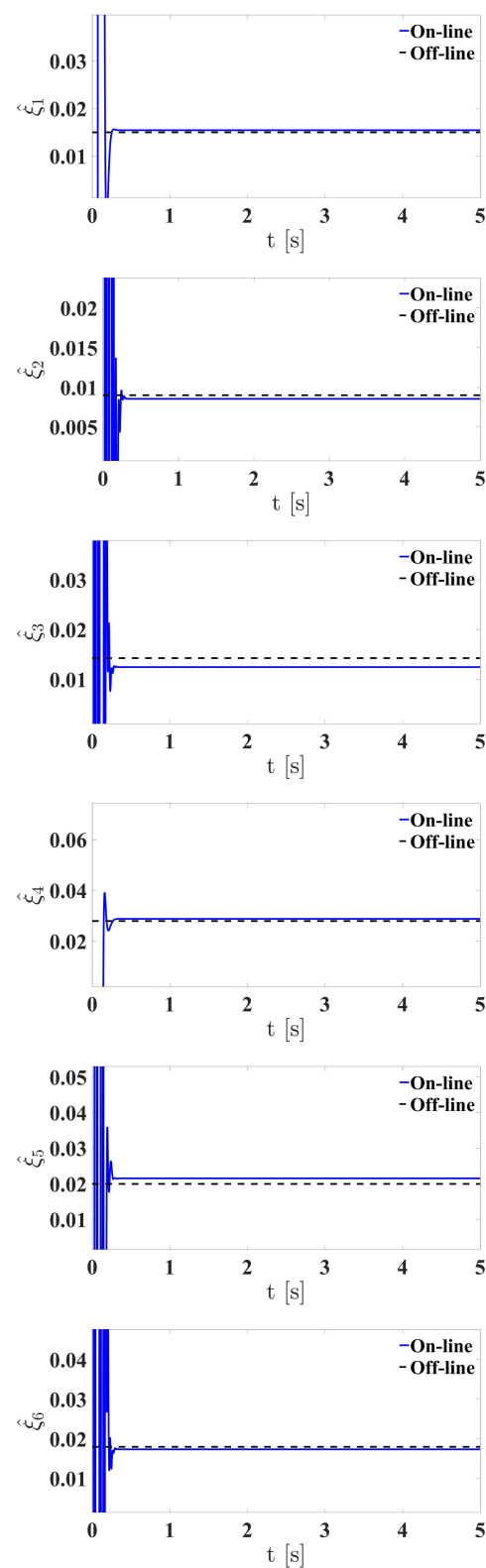**Figure 15.** Algebraic and on-line estimation of natural frequencies.

Figure 16. Algebraic and on-line estimation of damping ratios.

In the spectrogram shown in Figure 17, it is possible to observe that for $t > 18$ s, the frequency components of the signal vanish according to the slow and gradual decay in the velocity response.
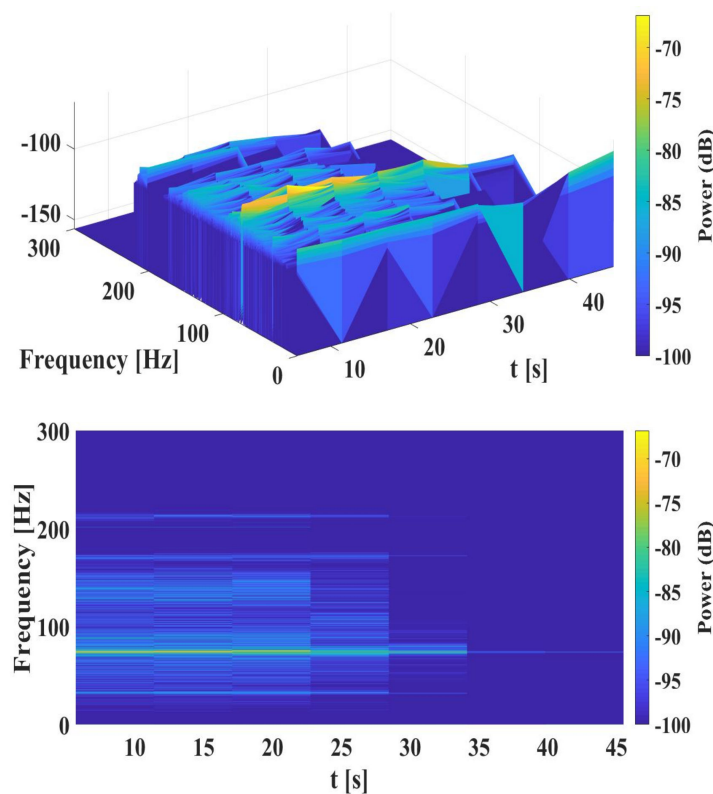
Figure 17. Spectrogram of the velocity measurements.

The dominant mode for this particular case (velocity measurements) is the one centred at 74 Hz, which is dominantly linear and time invariant for the particular turbulent wind speed of 20 m/s. The spectrogram shown in Figure 17 also reinforces the conclusion of the linearity assumption of the dynamic behaviour of the blade in those wind speed conditions, numerically quantified by the evaluated non-linearity index defined by (27) and the numeric result given by (29).

5. Conclusions

We proposed and evaluated an algebraic identification approach for the on-line estimation of the natural frequencies and damping ratios for an experimental case study of a particular wind turbine blade. We computed the natural frequencies and damping ratios based on the coefficients of the characteristic polynomial.

We used only measurements of a single velocity output or test location for the construction of the on-line algebraic estimator. It is important to mention that the approach presented can be easily extended for situations where acceleration measurements are preferred, since the characteristic polynomial is the same for both cases. The algebraic modal parameter identification method was evaluated on a wind turbine blade in a wind tunnel facility, excited by a turbulent wind flow that produces a change of its initial position and condition. The non-linearity indicator tested is easy to program and test for having a numeric and graphic indicator of the effects of the non-linearities present in the system due to its inner nature, e.g., construction based on composed materials, geometric non-linearities, etc.

On the other hand, it is necessary to carry out a precise analysis of the numerical methods applied to the original data to have a more rational criterion for the final determination of the presence of non-linearities; that is, care must be taken when defining an acceptable value of η to consider the system as non-linear. Here, we have assumed a value of $\eta \leq 0.9$ to establish that a given system is dominantly non-linear.

Abbreviations

The following abbreviations are used in this manuscript:

FRF	Frequency response function
$\mathcal{H}$	Hilbert transformation operator
RFP	Rational fractional polynomial
η	Principal Cauchy Value
dof	degree of freedom
ω_{ni}	Natural frequency of the ith mode or resonance
ξ_i	Damping ratio of the ith mode or resonance
s	Complex variable $s = j\omega$

References

1. Larsen, G.C.; Hansen, M.H.; Baumgart, A.; Carlén, I. *Modal Analysis of Wind Turbine Blades*; Forskningscenter Risoe: Risoe, Denmark, 2002.
2. He, J.; Fu, Z.F. *Modal Analysis*; Butterworth-Heinemann: Oxford, UK, 2001.
3. Heylen, W.; Lammens, S.; Sas, P. *Modal Analysis, Theory and Testing*; Katholieke Universiteit: Leuven, Belgium, 1998.
4. Zhou, W.; Chelidze, D. Generalized Eigenvalue Decomposition in Time Domain Modal Parameter Identification. *J. Vib. Acoust.* **2008**, *130*, 011001–011006. [CrossRef]
5. Chakraborty, A.; Basu, B.; Mitra, M. Identification of modal parameters of a mdof system by modified L-P wavelet packets. *J. Sound Vib.* **2006**, *295*, 827–837. [CrossRef]
6. Jezequel, L. Three New Methods of Modal Identification. *J. Vib. Acoust. Stress Reliab.* **1986**, *108*, 17–25. [CrossRef]
7. Garcia-Perez, O.; Silva-Navarro, G.; Peza-Solis, J. Flexible-link robots with combined trajectory tracking and vibration control. *Appl. Math. Model.* **2019**, *70*, 285–298. [CrossRef]
8. Beltran-Carbajal, F.; Silva-Navarro, G. Output feedback dynamic control for trajectory tracking and vibration suppression. *Appl. Math. Model.* **2020**, *79*, 793–808. [CrossRef]
9. Lim, T.W.; Cabell, R.H.; Silcox, R.J. On-Line Identification of Modal Parameters Using Artificial Neural Networks. *J. Vib. Acoust.* **1996**, *118*, 649–656. [CrossRef]
10. Isermann, R.; Munchhof, M. *Identification of Dynamic Systems*; Springer: Berlin, Germany, 2011.
11. Caldwell, R.A.; Feeny, B.F. Output-Only Modal Identification of a Nonuniform Beam by Using Decomposition Methods. *J. Vib. Acoust.* **2014**, *136*, 041010. [CrossRef]
12. Peeters, B.; Roeck, G.D. Stochastic System Identification for Operational Modal Analysis: A Review. *J. Dyn. Syst. T ASME* **2001**, *123*, 659–667. [CrossRef]
13. Scussel, O.; da Silva, S. Output-Only Identification of Nonlinear Systems Via Volterra Series. *J. Vib. Acoust.* **2016**, *138*, 041012–041013. [CrossRef]
14. Yang, Y.; Nagarajaiah, S. Output-only modal identification with limited sensors using sparse component analysis. *J. Sound Vib.* **2013**, *332*, 4741–4765. [CrossRef]
15. Kerschen, G.; Lenaerts, V.; Marchesiello, S.; Fasana, A. A Frequency Domain Versus a Time Domain Identification Technique for Nonlinear Parameters Applied to Wire Rope Isolators. *J. Dyn. Syst. T ASME* **2000**, *123*, 645–650. [CrossRef]
16. Kerschen, G.; Worden, K.; Vakakis, A.F.; Golinval, J.C. Past, present and future of nonlinear system identification in structural dynamics. *Mech. Syst. Signal Process.* **2006**, *20*, 505–592. [CrossRef]
17. Ondra, V.; Sever, I.A.; Schwingshackl, C.W. A method for detection and characterisation of structural non-linearities using the Hilbert transform and neural networks. *Mech. Syst. Signal Process.* **2017**, *83*, 210–227. [CrossRef]
18. Tomlinson, G. Developments in the use of the Hilbert transform for detecting and quantifying non-linearity associated with frequency response functions. *Mech. Syst. Signal Process.* **1987**, *1*, 151–171. [CrossRef]
19. Fliess, M.; Sira-Ramírez, H. An algebraic framework for linear identification. *ESAIM Control Optim. Calc. Var.* **2003**, *9*, 151–168. [CrossRef]
20. Beltran-Carbajal, F.; Silva-Navarro, G. On the algebraic parameter identification of vibrating mechanical systems. *Int. J. Mech. Sci.* **2015**, *92*, 178–186. [CrossRef]
21. Mikusiński, J. *Operational Calculus*; PWN and Pergamon: Warsaw, Poland, 1983.

22. Hu, Z.X.; Huang, X.; Wang, Y.; Wang, F. Extended Smooth Orthogonal Decomposition for Modal Analysis. *J. Vib. Acoust.* **2018**, *140*, 041008–041012. [CrossRef]

23. Basseville, M.; Benveniste, A.; Goursat, M.; Hermans, L.; Mevel, L.; der Auweraer, H.V. Output-Only Subspace-Based Structural Identification: From Theory to Industrial Testing Practice. *J. Dyn. Syst. T ASME* **2001**, *123*, 668–676. [CrossRef]

24. Vu, V.; Thomas, M.; Lafleur, F.; Marcouiller, L. Towards an automatic spectral and modal identification from operational modal analysis. *J. Sound Vib.* **2013**, *332*, 213–227. [CrossRef]

25. Beltran-Carbajal, F.; Silva-Navarro, G. Algebraic Parameter Identification of Multi-Degree-of-Freedom Vibrating Mechanical Systems. In *Proceedings of the 20th International Congress on Sound and Vibration (ICSV20)*; International Institute of Acoustics and Vibration: Bangkok, Thailand, 2013; pp. 1–8.

26. Beltran-Carbajal, F.; Silva-Navarro, G.; Trujillo-Franco, L.G. Evaluation of On-Line Algebraic Modal Parameter Identification Methods. In *Topics in Modal Analysis II*; Allemang, R., Ed.; Conference Proceedings of the Society for Experimental Mechanics Series; Springer: Cham, Switzerland, 2014; Volume 8, pp. 145–152.

27. Trujillo-Franco, L.G.; Silva-Navarro, G.; Beltran-Carbajal, F. Online Systems Parameters Identification for Structural Monitoring Using Algebraic Techniques. In *Dynamics of Civil Structures*; Caicedo, J., Pakzad, S., Eds.; Conference Proceedings of the Society for Experimental Mechanics Series; Springer: Cham, Switzerland, 2017; Volume 2, pp. 251–258.

28. Beltran-Carbajal, F.; Silva-Navarro, G.; Trujillo-Franco, L.G. On-line parametric estimation of damped multiple frequency oscillations. *Electr. Pow. Syst. Res.* **2018**, *154*, 423–432. [CrossRef]

29. Trujillo-Franco, L.G.; Silva-Navarro, G.; Beltran-Carbajal, F. On the modal parameters estimation in mechanical structures: A case study. In Proceedings of the 2017 14th International Conference on Electrical Engineering, Computing Science and Automatic Control (CCE), Mexico City, Mexico, 20–22 October 2017; pp. 1–6. [CrossRef]

30. Trujillo-Franco, L.G.; Silva-Navarro, G.; Beltran-Carbajal, F.; Campos-Mercado, E.; Abundis-Fong, H.F. On-Line Modal Parameter Identification Applied to Linear and Nonlinear Vibration Absorbers. *Actuators* **2020**, *9*, 119. [CrossRef]

31. Richardson, M.H.; Formenti, D.L. Parameter estimation from frequency response measurements using rational fraction polynomials. In *Proceedings of the 1st IMAC Conference*; Society for Experimental Mechanics: San Jose, CA, USA, 1982.

32. Kelly, L.G. Curve fitting and data smoothing. In *Handbook of Numerical Methods and Application*; Addison-Wesley: New York, NY, USA, 1967; Chapter 5.

33. Pastor, M.; Binda, M.; Harčarik, T. Modal Assurance Criterion. *Proc. Eng.* **2012**, *48*, 543–548. [CrossRef]

34. Vita, G.H.; Hemida, T.A.; Baniotopoulos, C.C. Generating atmospheric turbulence using passive grids in an expansion test section of a wind tunnel. *J. Wind Eng. Ind. Aerod.* **2018**, *178*, 91–104. [CrossRef]